Physical and Constitutive Modelling to Simulate Jointed Rock Mass under Uniaxial Stress State

Mahendra Singh*
K. Seshagiri Rao**

**Department of Civil Engineering*
IIT Roorkee, Roorkee- 247 667, INDIA
Email: singhfce@iitr.ernet.in

Department of Civil Engineering
IIT, Hauz Khas, New Delhi- 110 016, INDIA
Email: raoks@civil.iitd.ernet.in

ABSTRACT

Many of the engineering structures like foundations of bridge piers, towers and dams are located at shallow depth. The jointed rock mass beneath such near surface structures deforms under unconfined stress conditions. Joints, the most commonly occurring discontinuities, dominate the engineering response of the mass, as the normal stress acting on the joints is very low. Jointed rock mass fails in several modes and dilation occurs due to roughness and interlocking of the joints. Understanding of the failure mechanism of the mass and the modelling of the stress-deformation behaviour is necessary for reliable analysis and design of the structures in such rock masses. An extensive experimental programme was planned and executed on specimens of jointed mass with varying degree of interlocking, orientation and the geometry of the joints. The tests were performed under unconfined state to allow the dilation and also to allow specimen freely adopt the failure mode. The paper discusses the details of the experimental programme and some of the results obtained. The Poisson's ratio of the rock under uniaxial loading condition is observed to be consistently more than 0.5 for most of the cases. A constitutive model is suggested to explain the stress-deformation behaviour. The model is based on the normal and shear stiffnesses of the joints. The stiffnesses are treated to be varying with normal stress. The applicability of the constitutive model to the results of the experimental programme is also discussed.

Key words: Jointed rock mass, normal and shear stiffness, deformation, constitutive model.

1 INTRODUCTION

The rock masses encountered in civil and mining engineering projects are invariably jointed. Under unconfined or low confining pressure condition, the deformability of these masses is governed by both the properties of the joints and the intact rock material. The important properties of the joints affecting the mass behaviour are their

shear strength including dilation, stiffness, orientation, frequency and interlocking conditions. The analytical studies on these aspects have been conducted by many researchers in the past e.g. Goodman (1976), Goodman et al. (1968), Hart et al.(1988) and Shi (1988). The "Equivalent Continuum Material" approach has been found to be more convenient for the masses, which are highly fractured. The approach has been used by several investigators e.g. Gerrard (1982), Yoshinaka and Yamabe (1986), Huang et al. (1995), Singh (2000) and Li (2001). The closed form expressions for the equivalent deformation modulus have been given by Huang et al. (1995) and Li (2001). The expressions for constitutive equations by Huang et al. (1995) were derived for three sets of joints with two dominating sets symmetrically oriented about the direction of loading. However, Li (2001) derived the equations for one set of joints and neglected the dilation.

In the present study, an experimental programme was executed wherein jointed specimens simulating a jointed rock mass were tested under variable conditions of orientation and interlocking of joints (Singh, 1997). The specimens have been tested under uniaxial compression exhibiting typical modes of failure occurring in nature. The expressions for constitutive equations have been derived to compute the tangent modulus and lateral deformation of the jointed mass. The expressions take into account more than one set of joints at any arbitrary orientation and the effect of the dilation is considered through a dilatancy factor. The normal and shear stiffnesses used in the constitutive equations are treated to be varying with applied stress level. The applicability of the constitutive equations to the experimental results is also discussed in the study.

1.1 Earlier Model Studies on Jointed Rocks and Scope of Study

One of the best ways to investigate the mechanism of failure of jointed rocks is to conduct physical model study. The failure modes are found to have great influence on the response of the mass (Singh et al., 1997). The earlier studies have been conducted under direct shear, uniaxial, and triaxial stress conditions and some of these have been by Goldstein et al. (1966), Hayashi (1966), Brown (1970a, 1970b), Brown and Trollope (1970), Ladanyi and Archambault (1972), Einstein and Hirschfeld (1973), Lama (1974), Yaji (1984), Arora (1987), Roy (1993), and Yang and Huang (1995). Very few of these studies were conducted under the uniaxial stress conditions; rest were a part of experimental programme mainly directed towards confined conditions. Moreover, most of these studies have not been conducted on scale free jointed mass. The mass can be considered scale free, if it has more than about 150 blocks or at least 5 elements in each direction. These investigations are as such not adequate to understand the failure mechanism of mass under unconfined state where joints act under very low normal stress and the dilation plays an important role. The present study has therefore, been directed to study the strength and deformational behaviour of scale free jointed mass under unconfined condition.

2 EXPERIMENTAL PROGRAMME

Keeping the above points under consideration, the following specific experimental studies were planned and executed on the sand-lime brick model material:

(i) Tests were performed on specimens of jointed rock mass under unconfined conditions. A rock like model material (sand-lime brick) was used to simulate the weak rock. The specimens had at least six elements in each direction to behave free of scale effects.

(ii) The specimens had three sets of intersecting orthogonal joints (Fig. 1). The joint Set-I was continuous and the joints in this set were inclined at angles θ with the horizontal. The orientation θ was varied from 0° to 90°.

(iii) The joint set-II was orthogonal to joint set-I and stepped at variable stepping 's'. For each orientation, the stepping was varied from 0 to 7/8 of the width of the block at small intervals. The variation of stepping introduces changes in interlocking conditions. The joint set-III was always kept vertical (Type-A specimens, Fig. 1).

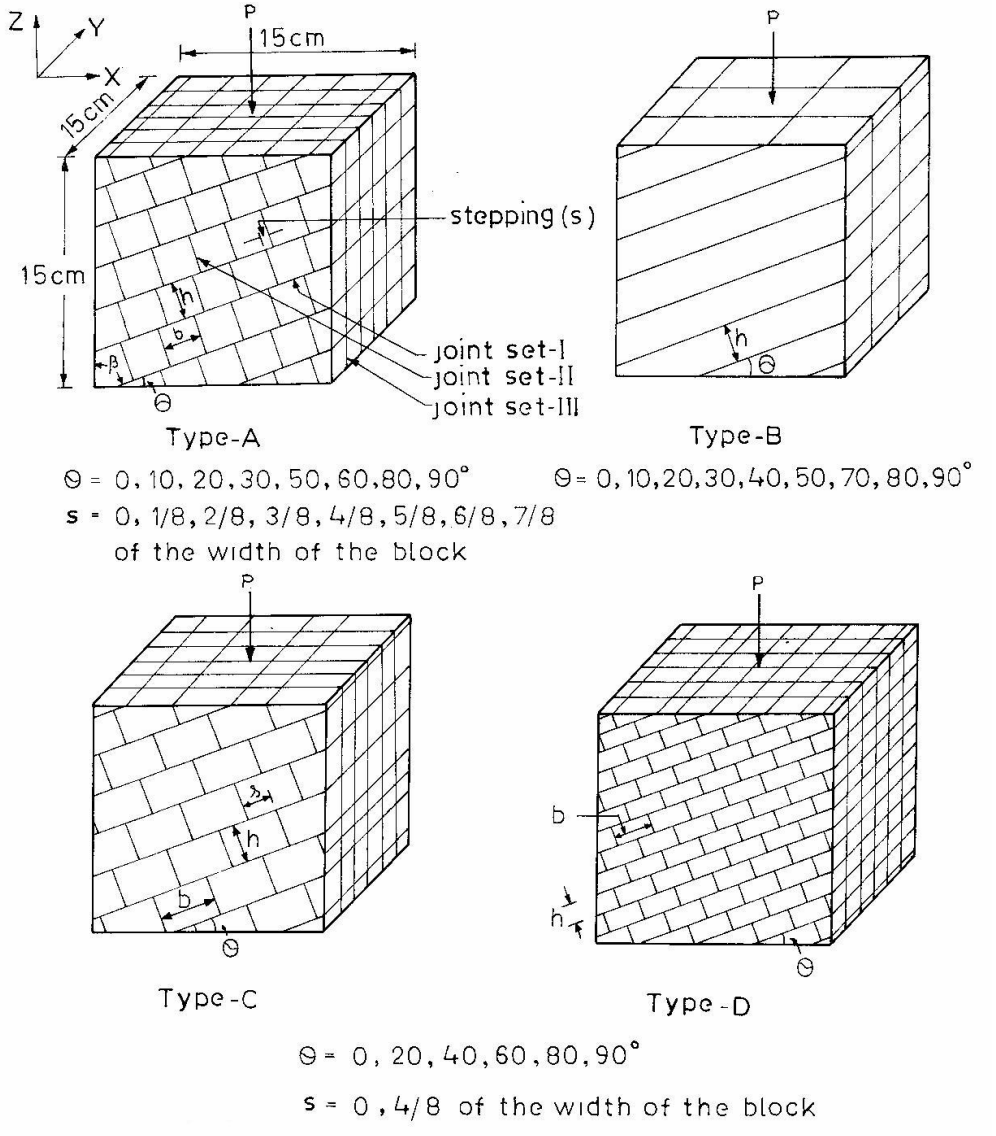

Fig. 1 - Configuration of various specimen with the joint sets

(iv) A few tests were also planned with changed geometry of blocks forming the specimens for selected orientations and steppings (Types B, C and D specimens, Fig. 1).
(v) Platens of size 15cm x 15cm were used at the top and the bottom of the specimen to distribute load uniformly.
(vi) Sandwiches of Teflon sheets smeared with silicon grease were used at the top and the bottom of the specimen to ensure friction free end loading system. Horizontal and vertical deformations were recorded with incremental load. The mode of failure of each specimen was recorded after the test.

3 RESULTS AND DISCUSSIONS

3.1 Model Material

The physical and engineering properties of the intact material are presented in Table 1. The average uniaxial compressive strength, σ_{ci}, of the sand-lime brick material is 17.13 MPa. The ratio of uniaxial compression to tensile strength for the present material is 6.8. The stress-strain curve for the intact material is presented in Fig. 2; the curve is elastic-plastic in nature with the failure strain about 0.5%. The tangent modulus E_i at 50% of failure stress is 5344 MPa. The modulus ratio (E_i/σ_{ci}) of the material is 312 and on Deere-Miller (1966) classification chart the material is classified as 'EM'.

Table 1- Physical and engineering properties of model material

Property	Value
Dry density, γ_d(kN/m^3)	16.86
Porosity (%)	36.94
UCS, σ_{ci} (MPa)	17.13
Brazilian strength,σ_{ti} (MPa)	2.49
Tangent modulus, E_i (GPa)	5.34
Poisson's ratio, ν_o	0.19
Cohesion, c_i (MPa)	4.67
Friction angle of intact material, $\phi_i°$	33.00
Friction angle along the Joints, $\phi_j°$	37.00
Deere-Miller classification (1966)	EM

The Mohr-Coulomb parameters c_i and ϕ_i for the intact material were determined by conducting triaxial shear strength tests under σ_3 = 0.98, 1.82, 2.89 and 4.07 MPa. The Mohr envelope for the intact material is presented in Fig. 3. The specimens failed in brittle manner under uniaxial loading and showed ductility with increase in confining pressure. The XRD analysis of the material indicated 64% Quartz, 14% Calcite, 11% Mica and 5.5% of Kaolinite and Feldspars each.

3.2 Modes of Failure of the Jointed Mass

The modes of failure of the jointed mass were very complex. There was always a combination of more than one failure mechanisms and single mode of failure was rarely found solely responsible for the entire failure. It was however, possible to

identify the most dominating mode initiating the failure of the specimen. Out of all combinations available, four distinct modes were identified as (i) *splitting* by vertical fracture planes passing through intact material, (ii) *shearing* through intact material, (iii) *rotation* of blocks and (iv) *sliding* along the critical joint planes. The typical specimens failed due to different modes are shown in Figs. 4 to 7.

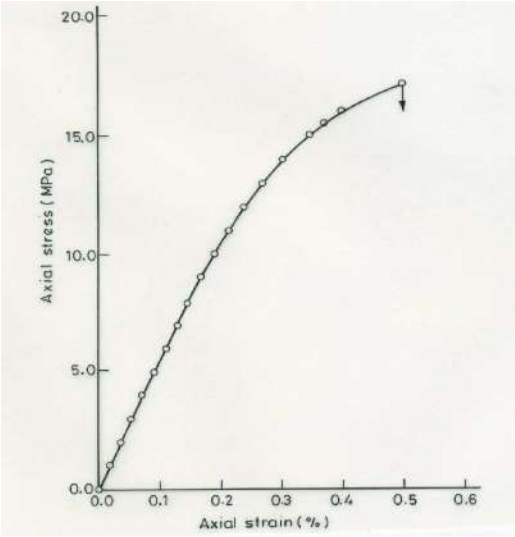

Fig. 2 - Stress-strain curve for intact model material

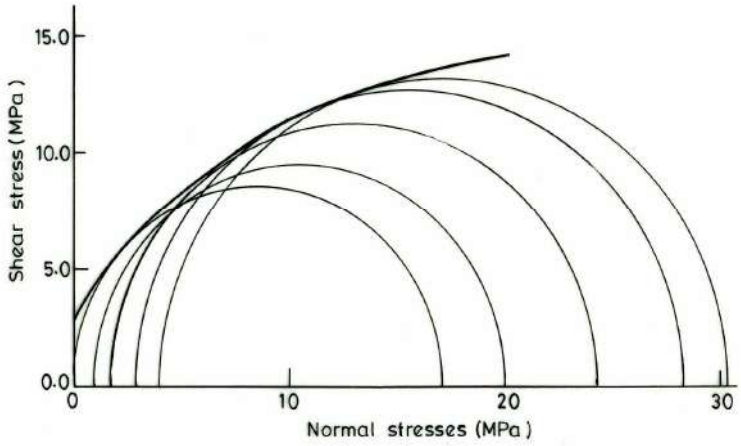

Fig. 3 - Mohr envelopes for the intact model material

3.2.1 Observations on modes of failure

The summary of failure modes occurring for various combinations of stepping and orientation for type-A specimens is presented in Table 2a. The modes of failure observed for Types-B, C and D specimens confirm to Table 2b. It is observed that a particular mode of failure lies in specific range of orientation of continuous joints and stepping. The shifting of mode from sliding to shearing and splitting for low θ values indicate that the various steppings used in this study correspond to different levels of interlocking of the mass.

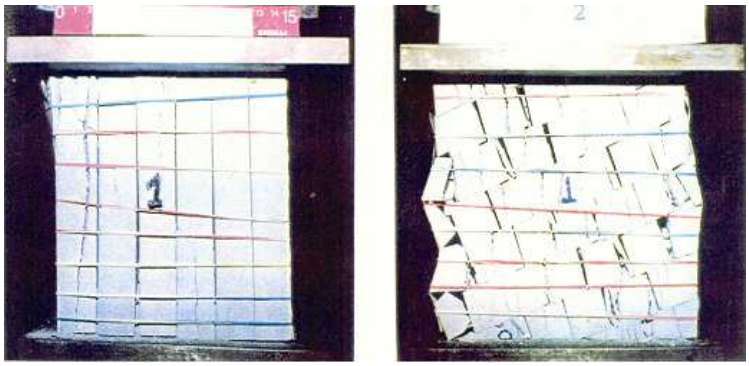

Fig. 4 - Typical specimens failed due to splitting

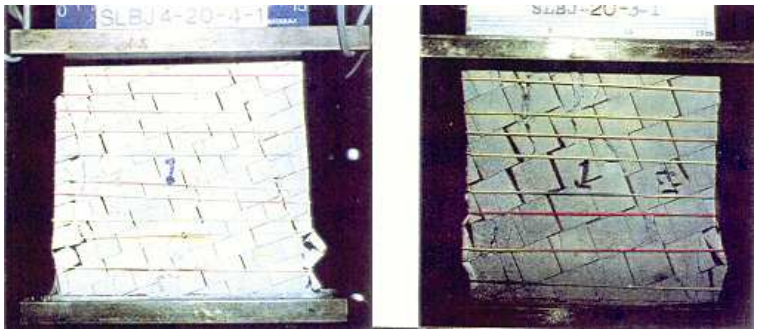

Fig. 5 - Typical specimens failed due to shearing

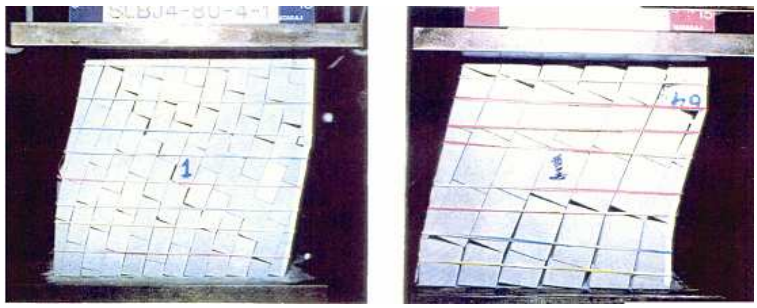

Fig. 6 - Typical specimens failed due to rotation

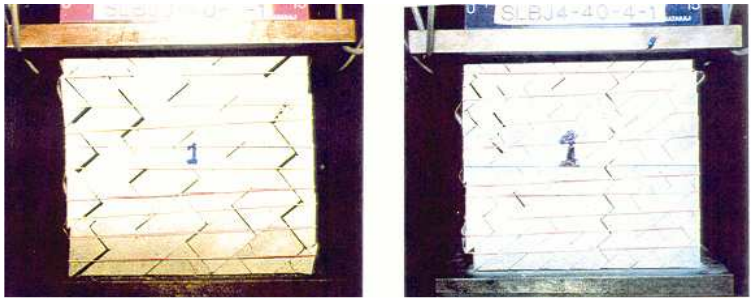

Fig. 7 - Typical specimens failed due to sliding

A rough estimate of the probable mode of failure of jointed rock mass under unconfined state in the field can be made on the basis of test results presented in Tables 2a and 2b as suggested in Table 3. It is assumed that the mass has two sets of joints, out of which one is continuous and the other is at low, intermediate or high level of interlocking as per the assessment of investigator in the field.

Table 2a – Summary of modes of failure for type-A specimens

θ°	Steppings							
	0	1/8	2/8	3/8	4/8	5/8	6/8	7/8
0	SHR+ SPL	SHR+ SPL	SPL	SPL	SPL	SPL	SPL	SHR+ SPL
10	ROT	SLD	SHR	SHR	SHR	SHR	SPL	SPL
20	SLD	SLD	SLD	SHR+ SPL	SHR+ SPL	SPL	SPL	SPL+ SHR
30	SLD	SLD	SLD	SLD	SLD+ ROT	SHR	SHR	SHR+ SPL
40	---	---	---	---	---	---	---	---
50	SLD	SLD	SLD	SLD	SLD	SLD	SLD	SLD
60	SLD	SLD	SLD	SLD	SLD	SLD	SLD	SLD
70	---	---	---	---	---	---	---	---
80	ROT	ROT	ROT	ROT	ROT	ROT	ROT	ROT
90	SHR+ SPL	SPL+ SHR	SHR	SHR	SHR	SHR	SHR	SPL+ SHR

SPL-Splitting through the intact material; SHR-Shearing of the intact material; ROT- Rotation; SLD-Sliding along the critical joints.

Table 2b - Summary of modes of failure for types B, C and D specimens

θ°	Type - B	Type - C		Type - D	
		s = 0	s = 4/8	s = 0	s = 4/8
0	SPL	SPL	SPL	SPL	SPL
10	SPL	-	-	-	-
20	SPL	SLD	SPL	SLD	SHR
30	SPL	-	-	-	-
40	SLD	SLD	SLD	SLD	SLD
50	SLD	-	-	-	-
60	-	SLD	SLD	ROT	SLD
70	ROT	-	-	-	-
80	ROT	ROT	ROT	ROT	ROT
90	SPL	SPL	SPL	SPL	SPL

Table 3 - Guideline for assessing failure mode

Orientation and interlocking condition	Failure Mode
$\theta = 0$ to $10°$	Splitting/ shearing
$\theta \approx 10°$, high interlocking	Splitting/ shearing
$\theta \approx 10°$, intermediate interlocking	Shifting from shearing to sliding
$\theta \approx 10°$, low / nil interlocking	Sliding
$\theta \approx 20°$, high interlocking	Shearing
$\theta \approx 20°$, intermediate interlocking	Shifting from shearing to sliding
$\theta \approx 0.8\ \phi_j$, high interlocking	Shifting from shearing to sliding
$\theta \approx 0.8\ \phi_j$, other than high interlocking	Sliding
$\theta \approx 0.8\phi_j$ to $65°$	Sliding
$\theta \approx 65°$ to $75°$	Shifting from sliding to rotation
$\theta \approx 75°$ to $85°$	Rotation
$\theta \approx 85°$ to $90°$	Shifting from rotation to shearing

3.3 Strength vs. Deformation Behaviour

The axial stress in the test specimen was computed by applying correction due to change in the cross sectional area during loading. The axial stress-deformation curves for some of the specimens tested are presented in Fig. 8. The curves are mostly in S shape. For almost all cases of splitting, shearing and rotation, smooth curves were obtained. In case of specimens failing due to sliding along the joints, stick slip phenomenon was observed for some cases and there was no well-defined peak load.

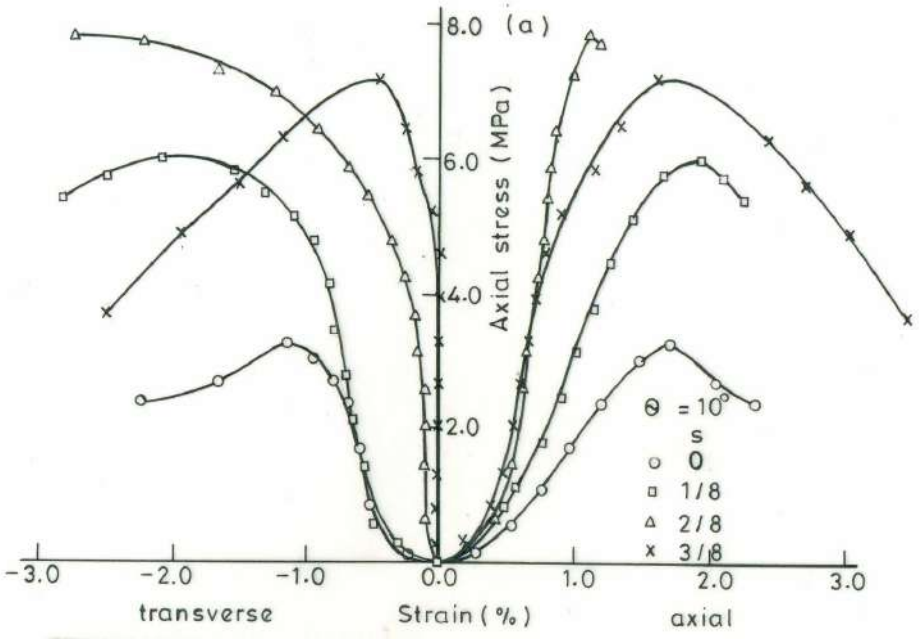

Fig. 8 - Axial stress vs deformation curves for some specimens

The experimental results on strength, tangent modulus, failure strain and Poisson's ratio are presented in Figs. 9 to 12 respectively. The strength is taken as the peak stress and the tangent modulus is computed by drawing tangent to the stress-deformation curve at 50% of peak stress. The strength and tangent modulus values are shown as percent of the respective values for intact model material. Following observation are made from these results:

- The mass behaves highly anisotropically in strength as well as deformational behaviour.
- The stepping increases the strength and tangent modulus in the range $\theta \leq 30°$. It may be noted that this is the range of orientation in which maximum variation in failure mode is observed. The engineering behaviour of the rock mass is therefore correlated with the failure mode which in turn depends on combination of θ and s.
- For $\theta > 30°$, there is no substantial effect of stepping on strength and tangent modulus.
- Failure strains also behave anisotropically and are failure mode dependent.
- The Poisson's ratio for most of the specimens is found to be higher than 0.5 and ranging upto 2.79. In literature, Lögters and Voort (1974) have also reported for actual rock mass tested by them in the field, the value of Poisson's ratio as high as 2.77. The extremely high value of Poisson's ratio was attributed by the authors to opening of joints when they were near critical orientation. Under confined state

the Poisson's ratio is likely to reduce and become less than 0.5 due to reduction in shear stresses and sliding along the joints.

A detailed elaboration on how to assess the strength and tangent modulus of the rock mass in the field is presented in elsewhere (Singh et al., 2002). The modelling of stress vs strain or deformation is presented in the following paragraphs.

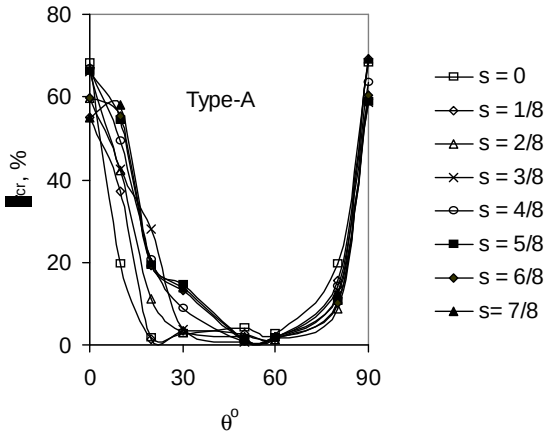

Fig. 9a - Values of strength (σ_{cr}, %) for type-A specimens

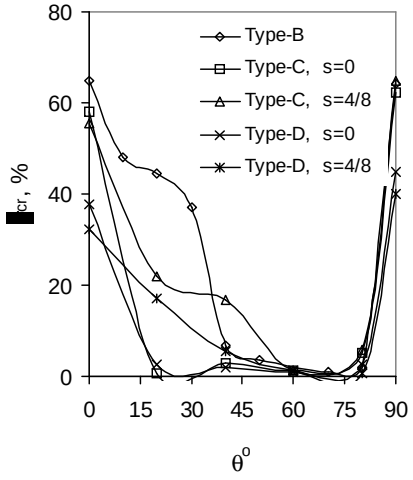

Fig. 9b - Values of strength (σ_{cr}, %) for type-B, C and D specimens

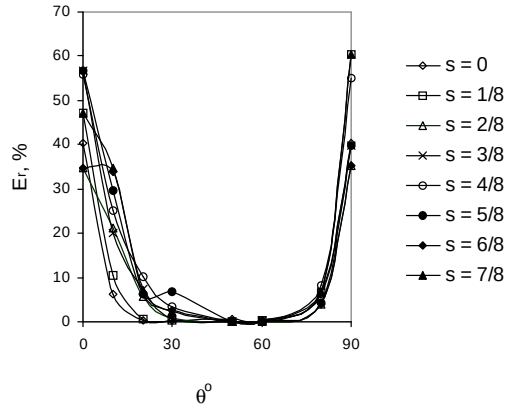

Fig. 10a - Values of tangent modulus (E_r, %) for type-A specimens

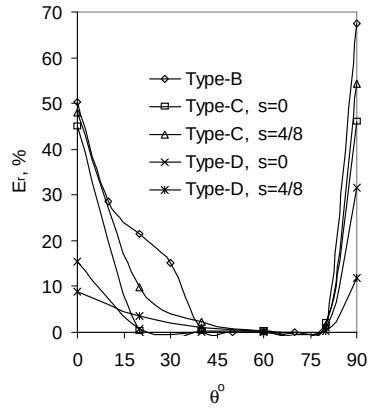

Fig. 10b - Values of tangent modulus (E_r, %) for type-B, C and D specimens

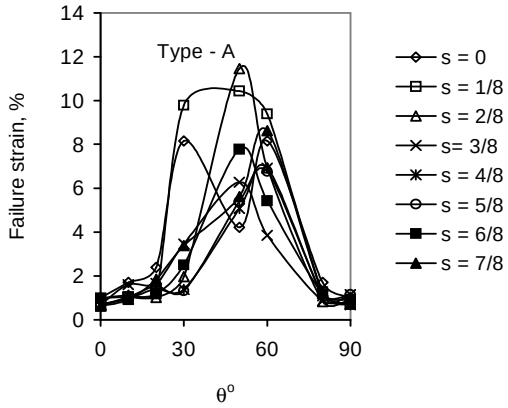

Fig.11a - Failure strains in axial direction for type- A specimens

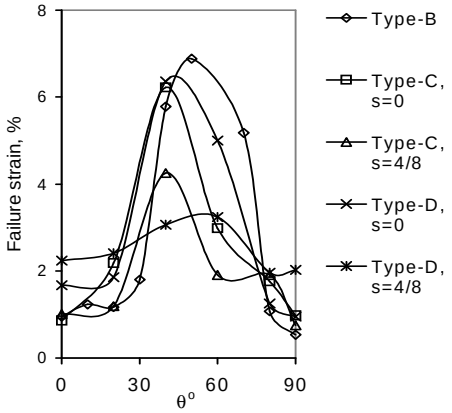

Fig.11b - Failure strains in axial direction for type-B, C and D specimens

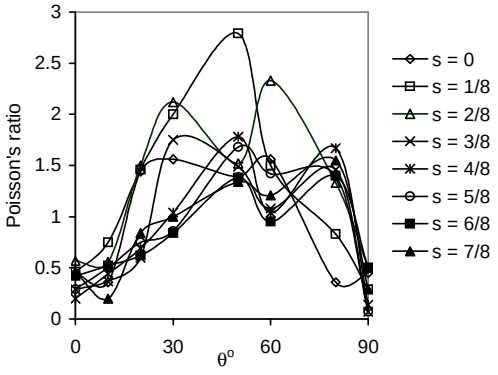

Fig. 12a - Poisson's ratio for type-A specimens

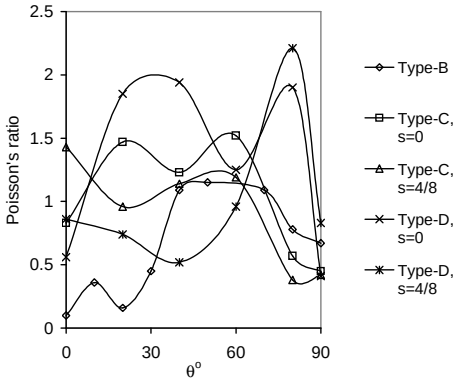

Fig. 12b - Poisson's ratio for type-B, C and D specimens

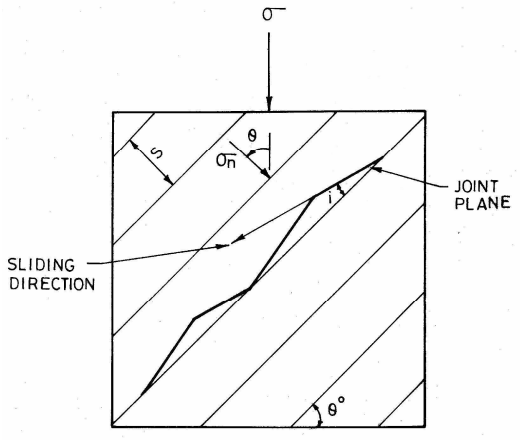

Fig.13 - A jointed mass with single dilatant joint

4 MODELLING OF STRESS-DEFORMATION RESPONSE

4.1 Constitutive Model

An empirical approach to derive the stress-strain curve without considering the mechanics involved, has been given by Singh et al. (1998). This approach was based on experimental results and fitting of the best curve. A slip based mechanistic model as used by Huang et al. (1995) is developed here.

Consider a jointed mass under uniaxial loading, with 'm' numbers of joint sets in the mass. The spacing of joints in j^{th} set is 'S_j' and the loading direction makes an angle θ_j with the normal to the joint plane (Fig. 13). Due to dilation, the sliding is at an inclination 'i' with the joint plane. The incremental values of normal and shear stresses $\Delta\sigma_{nj}$ and $\Delta\tau_j$, corresponding to the elemental increase in applied stress $\Delta\sigma$, on one joint of the j^{th} set will be:

$$\Delta\sigma_{nj} = \Delta\sigma \cos^2\theta_j \tag{1}$$

$$\Delta\tau_j = \Delta\sigma \sin\theta_j \cos\theta_j \tag{2}$$

For one joint, the corresponding incremental normal, shear and dilatational displacements respectively, will be

$$\Delta d_{nj} = \frac{\Delta\sigma_{nj}}{k_{nj}} = \frac{\Delta\sigma_j \cos^2\theta_j}{k_{nj}} \tag{3}$$

$$\Delta d_{sj} = \frac{\Delta\tau_j}{k_{sj}} = \frac{\Delta\sigma_j \sin\theta_j \cos\theta_j}{k_{sj}} \tag{4}$$

$$\Delta d_{dj} = \Delta d_{sj} \tan i = \Delta d_{sj}\, \lambda \tag{5}$$

where k_{nj} and k_{sj} are the normal and shear stiffnesses of the joint respectively and depend upon on the level of normal stress acting on the joint plane and λ is dilatancy factor = tan i.

For Axial Direction

The total displacement due to one joint in the direction of loading is given as follows:

$$\Delta d_{jz} = \Delta d_{nj} \cos\theta_j + \Delta d_{sj} \sin\theta_j - \Delta d_{dj} \cos\theta_j$$

$$\Rightarrow \Delta d_{jz} = \Delta\sigma_j \cos\theta_j \left[\frac{\cos^2\theta_j}{k_{nj}} + \frac{\sin^2\theta_j}{k_{sj}} - \frac{\lambda \sin\theta_j \cos\theta_j}{k_{sj}} \right] \quad (6)$$

If the length of the block of jointed mass in the direction of loading is L, the total displacement in the direction of loading, due to all the joints of j^{th} set will be:

$$\sum\left(\Delta d_{jz}\right) = \frac{\Delta\sigma_j L}{S_j} \cos^2\theta_j \left[\frac{\cos^2\theta_j}{k_{nj}} + \frac{\sin^2\theta_j}{k_{sj}} - \frac{\lambda \sin\theta_j \cos\theta_j}{k_{sj}} \right] \quad (7)$$

If E_o is the Young's modulus of the intact rock, the displacement of the intact rock in the direction loading will be

$$\Delta d_i = \frac{\Delta\sigma}{E_o} L \quad (8)$$

Summing up the displacements of the joints and the intact rock, the total displacement of the jointed mass will be

$$\Delta d_z = \frac{\Delta\sigma}{E_o} L + \frac{\Delta\sigma}{S_j} L \cos^2\theta_j \left[\frac{\cos^2\theta_j}{k_{nj}} + \frac{\sin^2\theta_j}{k_{sj}} - \frac{\lambda \sin\theta_j \cos\theta_j}{k_{sj}} \right] \quad (9)$$

The incremental axial strain $\Delta\varepsilon_z$ due to all the joint sets is given as:

$$\Delta\varepsilon_z = \frac{\Delta\sigma}{E_o} + \Delta\sigma \sum_{j=1}^{m} \frac{\cos^2\theta_j}{S_j} \left[\frac{\cos^2\theta_j}{k_{nj}} + \frac{\sin^2\theta_j}{k_{sj}} - \frac{\lambda \sin\theta_j \cos\theta_j}{k_{sj}} \right] \quad (10)$$

The equivalent deformation modulus of the jointed mass is given by the following expression.

$$\frac{1}{E_z} = \frac{1}{E_o} + \sum_{j=1}^{m} \frac{\cos^2\theta_j}{S_j} \left[\frac{\cos^2\theta_j}{k_{nj}} + \frac{\sin^2\theta_j}{k_{sj}} - \frac{\lambda \sin\theta_j \cos\theta_j}{k_{sj}} \right] \quad (11)$$

For Lateral Direction

Total displacement due to one joint in direction X:

$$\Delta d_{jx} = \Delta d_{nj} \sin\theta_j - \Delta d_{sj} \cos\theta_j - \Delta d_{dj} \sin\theta_j$$

$$\Rightarrow \Delta d_{jx} = \Delta\sigma_j \cos\theta_j \sin\theta_j \left[\frac{\cos\theta_j}{k_{nj}} - \frac{\cos\theta_j}{k_{sj}} - \frac{\lambda \sin\theta_j}{k_{sj}} \right] \quad (12)$$

Total dsiplacement due to all joints of j^{th} set in direction X is given by

$$\sum(\Delta d_{jx}) = \frac{\Delta\sigma L \cos^2\theta_j \sin\theta_j}{S_j} \left[\frac{\cos\theta_j}{k_{nj}} - \frac{\cos\theta_j}{k_{sj}} - \frac{\lambda \sin\theta_j}{k_{sj}} \right] \quad (13)$$

Strain in X direction due to lateral expansion of intact rock is $\nu_o(\Delta\sigma/E_o)$. The displacement due to one joint set, in transverse direction X is

$$B \frac{\nu_o \Delta\sigma}{E_o} + \frac{\Delta\sigma L \cos^2\theta_j \sin\theta_j}{S_j} \left[\frac{\cos\theta_j}{k_{nj}} - \frac{\cos\theta_j}{k_{sj}} - \frac{\lambda \sin\theta_j}{k_{sj}} \right]$$

where B is the dimension of the specimen in X direction.

The strain in direction X, due to all the joint sets will be

$$\Delta\varepsilon_x = \frac{\nu_o \Delta\sigma}{Eo} + \frac{\Delta\sigma L}{B} \sum_{j=1}^{m} \frac{\cos^2\theta_j \sin\theta_j}{S_j} \left[\frac{\cos\theta_j}{k_{nj}} - \frac{\cos\theta_j}{k_{sj}} - \frac{\lambda \sin\theta_j}{k_{sj}} \right] \quad (14)$$

4.2 Normal Stiffness

The normal stiffness of the joints was determined in the laboratory by loading them normal to their planes and then plotting the normal stress against the closure of the single joint. The bricks were cut into square plates of 2.5 cm thickness each. A set of six such plates kept one above the other was prepared and load was applied normal to the joints. The stress vs. deformation curve of this system up to failure was observed. The deformation of the intact material was subtracted to get the deformation of the joints. This deformation was divided by number of joints to get stress vs. deformation behaviour of the single joint (Fig. 14). It is observed that the stress required to cause unit closure increases exponentially with increasing deformation. A best fitting power law was used to describe the relation between the normal stress and the closure of the joint as follows.

$$\sigma_n = 253.14(\delta)^{2.36} \quad (15)$$

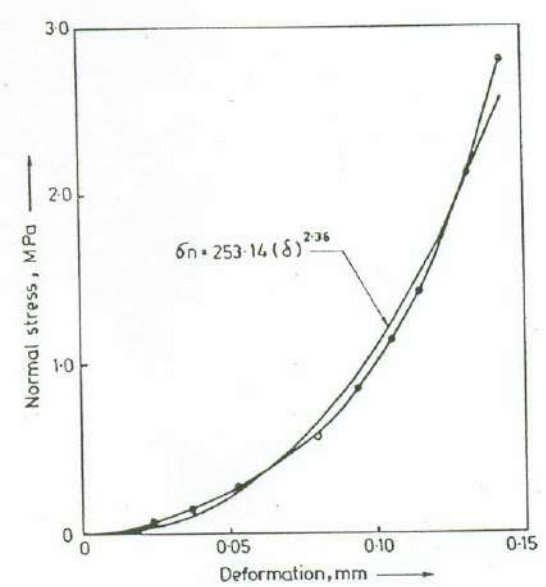

Fig.14 - Normal stress-deformation behaviour of single joint

By differentiating σ_n with respect to δ, the following expression was obtained for the normal stiffness.

$$k_n = 24.27\sigma_n^{0.42} \text{ MPa/mm} \quad (16)$$

where σ_n is normal stress in MPa and δ is normal closure of the joint in mm.

4.3 Shear Stiffness

The shear stiffness of the joints was determined by conducting direct shear tests on the joint surface and plotting shear stress against the shear deformation. Some researchers propose to use a constant value of the shear stiffness (Huang et al., 1995). Singh (2000) however observed that the shear stiffness varies with the level of applied stresses and proposed a model to account for the variation in the shear stiffness depending on the level of the applied stress (Fig. 15). This model is used to compute the shear stiffness in this study. As per this model the k_s is assumed as follows:

(i) for $0 \leq \sigma \leq 0.25\ \sigma_{cj}$; k_s =linearly varying from 0 to k_{smax},
(ii) for $0.25\sigma_{cj} \leq \sigma \leq 0.75\ \sigma_{cj;}$ $k_s = k_{smax}$, and
(iii) for $0.75\sigma_{cj} \leq \sigma \leq \sigma_{cj;}$ k_s= linearly varying from k_{smax} to 0.

where σ_{cj} = applied stress at failure under uniaxial loading condition. The value of k_{smax} for the joints in this study was observed to be 0.5886 MPa/mm.

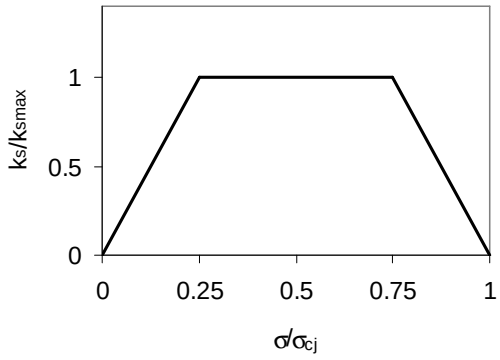

Fig.15 - Model for variation of k_s with uniaxial stress (Singh, 2000)

4.4 Applicability of the Model

The constitutive equations suggested above are applied to the experimental data obtained from the testing programme. Following are the input parameters for the model;

E_o = 5344 MPa; ν = 0.19; L = b = 150mm; k_{smax} = 0.5886 MPa/mm;
$k_n = 24.27\sigma_n^{0.42}$ MPa/mm

A computer programme was used to apply the model. The programme uses, up to the failure load, the incremental increase in applied uniaxial loading and computes the incremental deformations in Z and X directions and the incremental modulus at each step. Following sequence of computations is adopted.

- Read input data i.e. failure stress σ_1, E_o, ν, L, b, number of joint sets and $k_{smax.}$
- For each joint set read orientation θ_j, spacing S_j and the first trail value of λ.
- Compute incremental stress = 1/20 of the failure stress.
- Apply incremental load and compute incremental strains $\Delta\varepsilon_z$ and $\Delta\varepsilon_x$.
- For each incremental increase in loading, compute tangent modulus $E_z = \Delta\sigma/\Delta\varepsilon_z$. Record the value of E_z corresponding to the applied stress equal to half of the failure stress. Compare this modulus with experimental value.
- Choose another trial value of λ and repeat the steps (iv) and (v) till the experimental value of E_z matches with the experimental result.

The values of dilatancy factor λ giving best promising tangent modulus values are presented in Table 4. Following observations are made from this table.

Table 4- Dilatancy factor λ predicting closest tangent modulus

θ°	Stepping s							
	0	1/8	2/8	3/8	4/8	5/8	6/8	7/8
10	0.206	0.29	0.358	0.3556	0.367	0.3732	0.3794	0.3746
20	-1.41	-0.8	0.564	0.5804	0.6164	0.5655	0.5685	0.582
30	-1.88	-2.15	0.18	-0.13	0.7285	0.8135	0.643	0.638
50	0.0015	-7.2	-8.0	-10.5	-9.5	-4.3	-6.0	-4.6
80	0.2062	0.2245	0.103	0.2568	0.2808	0.1138	0.0925	0.2445

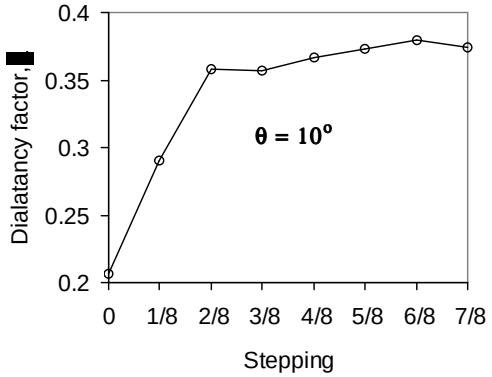

Fig. 16 - Variation of optimal λ with stepping for θ = 10°

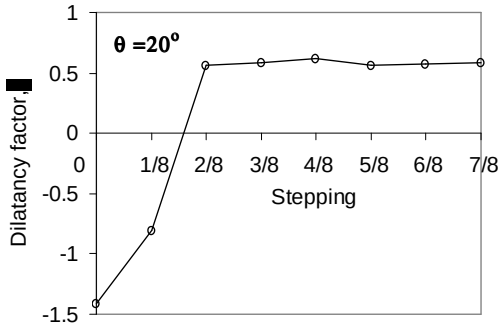

Fig. 17 - Variation of optimal λ with stepping for θ = 20°

4.4.1 For $\theta = 10^o$

It can be seen from Table 3, that most of the values of λ giving matching E_z lie between 0.206 and 0.3794. The variation of λ with stepping is shown in Fig. 16; it is seen that λ gradually increases from 0.206 (s = 0) to 0.358 (at s = 2/8) and after that remains almost constant (λ ≈ 0.37).

4.4.2 For $\theta = 20^o$

For s = 0 and s = 1/8, the values of λ to predict matching tangent modulus are negative (Fig. 17). We consider these negative values to be unrealistic as they indicate contraction of the jointed mass at failure. For stepping, s ≥ 2/8, there is not much variation in the value of λ. An average value 0.58 can be conveniently used to predict the modulus value close to those obtained experimentally. It is interesting to note that s = 0 and s = 1/8 represent cases of pure sliding and a possible explanation is given in subsequent discussion with other cases of sliding mode.

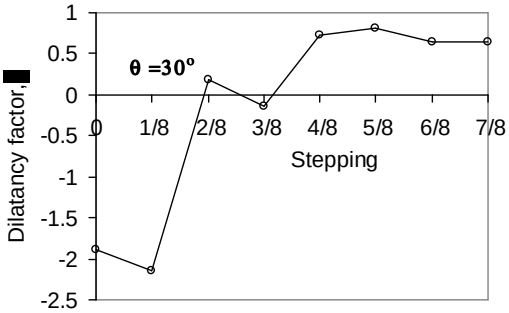

Fig. 18 - Variation of optimal λ with stepping for θ = 30°

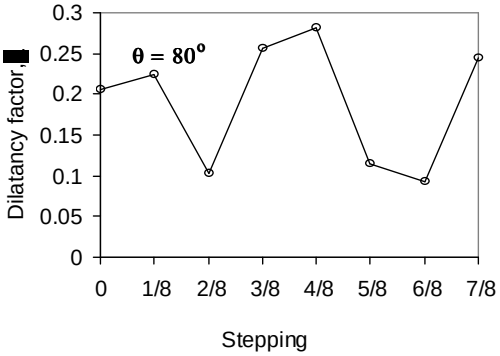

Fig. 19 - Variation of optimal λ with stepping for θ = 80°

4.4.3 For θ = 30°

For s = 0 to 3/8 (except 2/8), all optimal values of λ are negative. For s = 4/8, 5/8, 6/8 and 7/8 the values are positive. The variation of λ is shown in Fig. 18. These orientations exhibit the shearing mode of failure or a transition between sliding and shearing. An average value of λ for non-sliding cases may be taken as 0.71.

4.4.4 For θ = 50° and 60°

All the optimal values of λ are negative. The continuous joint set is inclined at angle more than friction angle of joints (ϕ_j = 37°). From mechanics point of view the specimens should fail due to their own weight. A small strength however is indicated by the experimental results. The reason for this strength is that after some deformation, the blocks introduce some kind of interlocking that gives rise to apparent cohesion and some strength is shown by the mass. The experimental results in fact are more indicative of the residual strength rather than the peak strength of the mass. Singh (2005) also observed during back analysis in some slopes that the cohesion increased with deformation. The constitutive model in its present form can not model these cases of residual strength.

4.4.5 For θ = 80°

For θ = 80°, the optimal λ fluctuates between 0.0925 and 0.2825 (Fig. 19). There is no trend of the λ values with the stepping. The failure mode for these specimens was rotation.

4.4.6 For θ = 0° and 90°

The basic assumption in the development of the constitutive model used here is that, there should be some slip along the joints. For θ = 0°, only the closure can take place and the dilation does not affect the result as it will have no component contributing axial strain. A constant value of the modulus is indicated for all the steppings, which is far less than the average value obtained experimentally. Similarly, for θ = 90°,

neither slip nor dilation is going to occur. The model in its present form therefore does not explain the behaviour of these orientations successfully.

5 CONCLUSIONS

For many civil engineering projects, the foundations rest on rocks at shallow depth. The rocks encountered are seldom intact and have discontinuities, most common of which are the joints. The assessment of the strength and deformability of such jointed rocks is always a challenging job before the designers. The behaviour is further complicated due to variety of modes of failure that can occur in unconfined state of jointed rocks. The present experimental programme has been aimed to have better understanding of occurrence of different mode of failure and their influence on the deformability of the mass under unconfined state. The study shows four distinct possible failure modes for jointed mass, i.e. splitting of intact material, shearing of intact material, rotation of blocks and sliding along the critical joints.

The expressions for a constitutive model have been suggested based on the slip along the joint surfaces. The model can be used for mass having any number of continuous joint sets at variable orientations. The effect of dilation and variability of the normal and tangential stiffnesses, on the deformability of the mass in longitudinal as well as in lateral directions can be studied through this model.

Following conclusions are drawn from the study.

- Contrary to popular belief, the Poisson's ratio of the dialatant jointed rock mass under uniaxial loading condition, is found to be consistently more than 0.5 for majority of the cases. This is due to opening of joints under very low normal stresses.
- A jointed rock mass having a single joint set at critical orientation ($\theta \approx 45°+\phi_j/2$) fails under its own weight. However if there are more than one joint sets, the corners of the blocks in the mass introduce some interlocking leading to apparent cohesion. The mass therefore has some strength even if the joints are critically oriented.
- Four distinct failure modes, i.e. splitting, shearing, rotation and sliding are possible for a jointed rock mass under uniaxial loading conditions.
- The failure mode depends on the orientation of joints with loading direction and interlocking of the mass. Assessment of the probable failure mode is possible based on the mapping of joints in the field and the judgement of the engineer about the interlocking of the mass.
- The deformational behaviour of the mass, when it fails due to sliding, shearing or splitting in the range $0 < \theta < \phi_j$, can best be modelled through the slip based constitutive model suggested in the study. The cases of $\theta = 0°$ and $90°$ cannot be modelled by the model in its present form.
- The dilatancy factor 'λ', can model the extent of interlocking of the mass. For the range $0 < \theta < \phi_j$, λ has specific trend and is related with the failure mode.

Acknowledgement

Some part of the work reported here has been taken from the PhD thesis of the first author that was completed by him under the supervision of Prof. T. Ramamurthy of IIT Delhi and Prof. K.S. Rao. The contributions of Prof. Ramamurthy in completion of the work are gratefully acknowledged.

References

Arora, V.K. (1987). Strength and Deformational Behaviour of Jointed Rocks., Ph.D. Thesis, IIT Delhi, India.

Brown, E.T. (1970a). Strength of Models of Rock with Intermittent Joints, Jl. of Soil Mech. & Found. Div., Proc. ASCE, 96(SM6), 1935-1949.

Brown, E.T. (1970b). Modes of Failure in Jointed Rock Masses, Proc. of the Second Cong. of ISRM, Belgrade, Vol-II, 293-298.

Brown, E.T. and Trollope, D.H. (1970). Strength of a Model of Jointed Rock, Jl. of Soil Mech. & Found. Div., Proc. ASCE, 96(SM2), 685-704.

Deere, D.U. and Miller, R.P. (1966). Engineering Classification and Index Properties for Intact Rock, Technical Report No. AFNI-RT-65-116. Air Force Weapons Laboratory, New Mexico.

Einstein, H.H. and Hirschfeld, R.C. (1973). Model Studies on Mechanics of Jointed Rock., Jl. of Soil Mech. & Found. Div. Proc. ASCE, 90, 229-248.

Gerrard, C.M. (1982). Equivalent Elastic Moduli of a Rock Mass Consisting of Orthorhombic Layers. Int. J. Rock Mech. Min. Sci. Geomech. Abstr. 1982; 19:9–14.

Goldstein, M., Goosev B., Pyrogovsky N., Tulinov R. and Turovskaya A. (1966). Investigation of Mechanical Properties of Cracked Rock., Proc Ist Cong., Int. Soc. Rock. Mech. Lisbon, 1, 521-524.

Goodman, R.E. (1976). Methods of Geological Engineering in Discontinuous Rocks. San Francisco: West Publishing Company, 1976.

Goodman, R.E., Taylor R.L. and Brekke T.L. (1968). A Model for the Mechanics of Jointed Rock. J. Soil Mech. & Found. Div. Proc. ASCE 94, SM3, 1968. 637–659.

Hart, R.D., Cundall, P.A., Lemos J.V. (1988). Formulation of a Three Dimensional Distinct Element Method—Part II: Mechanical Calculations for Motion and Interaction of a System Composed of Many Polyhedral Blocks. Int. J. Rock Mech. Min. Sci. Geomech. Abstr., 25(3), 117–25.

Hayashi, M., (1966). Strength and Dialatancy of Brittle Jointed Mass- The Extreme Value Stochastic and Anisotropic Failure Mechanism., Proc Ist Cong. ISRM, Lisbon, 1, 295-302.

Huang T.H., Chang C.S. and Yang Z.Y. (1995). Elastic Moduli for Fractured Rock Mass. Rock Mech. Rock Engng. 28(3), 135-144.

Ladanyi, B. and Archambault, G. (1970). Simulation of Shear Behaviour of a Jointed Rock Mass, Rock Mechanics- Theory and Practice, Proc. 11th Symp. Rock Mech., Berkeley, California, 105-125.

Ladanyi, B. and Archambault, G. (1972). Evaluation of Shear Strength of a Jointed Rock Mass., Proc. 24th Int. Geological Congress, Montreal, Section 13D, 249-270.

Lama, R.D. (1974). The Uniaxial Compressive Strength of Jointed Rock, Prof. L. Müller Festschrift, Inst. Soil Mech. & Rock Mech., Univ. Karlsruhe, Karlsruhe,

67-77.
Li, C. (2001). A Method for Graphically Presenting the Deformation Modulus of Jointed Rock Masses, Rock Mech. Rock Engng, 34(1), 67-75.
Lögters, G. and Voort, H. (1974). In-Situ Determination of the Deformational Behaviour of a Cubical Rock-Mass Sample under Triaxial Load, Rock Mechanics, 6, 65-79.
Roy, N. (1993). Engineering Behaviour of Rock Masses Through Study of Jointed Models., Ph.D. Thesis, IIT Delhi, India.
Shi, G. (1988). Discontinuous Deformation Analysis—A New Numerical Model for the Statics, Dynamics of Block Systems. PhD thesis, University of California, Berkeley, USA, 1988.
Singh, B. (2005) Personal Communication.
Singh, M. (1997). Engineering Behaviour of Jointed Model Materials, Ph.D. Thesis, IIT, New Delhi, India.
Singh, M. (2000). Applicability of a Constitutive Model to Jointed Block Mass, Rock Mech. Rock Engng., 33 (2), 141-147.
Singh, M., Rao, K.S. and Ramamurthy, T. (1997). Prediction of Strength of Jointed Rock Mass Based on Failure Mode, Proc. Indian Geotechnical Conference-1997, Vadodara, 139-142.
Singh, M., Rao, K.S. and Ramamurthy, T. (1998). A Simple Stress-Strain Curve For Jointed Block Mass, Proc. Indian Geotechnical Conference-1998, N. Delhi, 343-346.
Singh, M., Rao, K.S. and Ramamurthy, T. (2002). Strength and Deformational Behaviour of Jointed Rock Mass, Rock Mech. Rock Engng., 35(1), 45-64.
Yaji, R.K. (1984). Shear Strength and Deformation Response of Jointed Rocks., Ph.D. Thesis IIT Delhi, India.
Yang, Z.Y. and Huang, T.H. (1995). Effect of Joint Sets on the Anisotropic Strength of Rock Masses, Proc. 8th Cong. ISRM, Japan, 367-370.
Yoshinaka and Yamabe (1986). Evaluation of Mechanical Parameters of Rock Mass in Numerical simulation. Int. J. Rock Mech. Min. Sci. Geomech. Abstr. 23(1), 19–28.